AAPS PharmSciTech (2021) 22:1
DOI: 10.1208/s12249-020-01865-z

Research Article

Transdermal Delivery of Salmon Calcitonin Using a Dissolving Microneedle Array: Characterization, Stability, and *In vivo* Pharmacodynamics

Lu Zhang,[1] Yingying Li,[1] Fang Wei,[1] Hang Liu,[1] Yushuai Wang,[1] Weiman Zhao,[1] Zhiyong Dong,[1] Tao Ma,[1] and Qingqing Wang[1,2]

Received 13 September 2020; accepted 24 October 2020

Abstract. Salmon calcitonin (sCT) is a polypeptide drug, possessing the ability to inhibit osteoclast-mediated bone resorption. Just like other bioactive macromolecules, sCT is generally administered to the patients by either injection for poor compliance or through nasal spray for low bioavailability, which limits its use as therapeutic drugs. In the present study, to overcome the limitations of the conventional routes, two new dissolving microneedle arrays (DMNAs) based on transdermal sCT delivery systems were developed, namely sCT-DMNA-1 (sCT/Dex/K90E) and sCT-DMNA-2 (sCT/Dex-Tre/K90E) with the same dimension, meeting the requirements of suitable mechanical properties. An accurate and reliable method was established to determine the needle drug loading proportion in sCT-DMNAs. The stability study exhibited that the addition of trehalose could improve the stability of sCT in DMNA under high temperature and humidity. Further, *in vivo* pharmacodynamic study revealed that DMNA patch could significantly enhanced relative bioavailability to approximately 70%, and the addition of trehalose was found to be beneficial for sCT transdermal delivery. Therefore, sCT-DMNA is expected to replace traditional dosage form, providing a secure, efficient, and low-pain therapeutic strategy for bone disorders.

KEY WORDS: salmon calcitonin; dissolving microneedle array (DMNA); transdermal delivery; relative bioavailability; trehalose.

INTRODUCTION

Peptides and proteins have the advantages of high specificity and safety as therapeutic agents for different diseases (1). Unfortunately, their clinical applications are limited by the existing delivery methods. One such agent is salmon calcitonin (sCT) (2), an FDA-approved polypeptide drug, primarily used for treating Paget's disease, osteoporosis (3), malignant hypercalcemia (4), and the pain of bone metastasis (5). sCT can regulate the metabolism of calcium and phosphorus and reduce the activity of osteoclast (6). Moreover, it can minimize the loss of bone calcium and stimulate the proliferation and differentiation of osteoblasts. Additionally, it also possesses significant analgesic effect (2).

As a highly bioactive polypeptide molecule, sCT has a large molecular weight with complex spatial configuration, and it is prone to denaturation under the influence of temperature as well as acids/bases. The activity of sCT mainly depends on its spatial structure and amino acid sequence (7), a common characteristic of most biotechnological drugs, which indicates that maintaining the structural stability is an primary guarantee for the efficacy. To date, sCT is generally administered by clinical injections. However, this administration frequently causes large fluctuations of blood serum concentration level that could lead to the adverse side effects (8).

In recent years, the non-injection drug delivery systems administered through oral, transdermal, nasal, and rectal routes have attracted great attention from the medical community (9). Some polymer-based oral delivery systems of sCT have earlier been tested *in vivo*, where the polymers can protect sCT from the impact of the gastrointestinal pH environment for oral delivery system. However, these systems either could not improve the lower bioavailability of drug (10–12) or could cause gastrointestinal symptoms (13), including abdominal cramps.

In this context, it is to be mentioned here that the only sCT delivery system that has been successfully marketed is the nasal formulation of sCT. Although the nasal delivery avoids the impact of the adverse environment of the gastrointestinal tract, the poor bioavailability of sCT could limit its curative effects. Novartis Pharma Schweiz AG had produced nasal spray dosage form of sCT which is unable to meet the needs of clinical applications as it exhibited much lower bioavailability (approximately 3%) than that of injection (14). Moreover, the long-term use of nasal sprays could cause severe epistaxis and nasal

Lu Zhang and Yingying Li contributed equally to this work.

[1] School of Pharmacy, Bengbu Medical College, No. 2600, Donghai Avenue, Bengbu, 233000, Anhui, China.
[2] To whom correspondence should be addressed. (e–mail: qingqingwang@bbmc.edu.cn)

irritation (15). To enhance the nasal bioavailability of sCT, Amaro *et al.* developed sCT-loaded nanoporous/nanoparticulate microparticles (NPMPs). Even loaded with NPMPs, *in vivo* pharmacokinetic study in rats showed that the nasal absolute bioavailability of sCT was only 10.1 ± 1.37% (16). Therefore, it becomes highly imperative to design a new sCT delivery system with high bioavailability and biosafety, which could be administrated autonomously by patients. Herein, in the present study, instead of injection and nasal routes, transdermal administration has been proposed.

Tas *et al.* fabricated microneedles (MNs) with only five-needle arrays from stainless steel sheets, where each MN was 730 μm long, 180 μm wide at the base, 50 μm in thickness, and coated the surface of MNs with sCT to design the delivery system sCT-MNs (17). The authors demonstrated that the *AUC* (area under the curve) of sCT-MNs was not statistically different from intravenous injection, suggesting that the use of microneedle patch for sCT delivery could be a viable alternative to injection of sCT and other peptides or protein therapeutics. However, for this kind of sCT-MNs system, the dosage is limited by the coating thickness and the adhesive strength of coating to microneedle required to resist transdermal repulsion. Moreover, the inner stainless MNs may not only lead to skin allergy but also generate the sharp and biohazardous waste needles after administration.

Till now, dissolving microneedles (DMNs) exert more advantages for the delivery of peptide and protein drugs (18). The delivery system can be prepared by simply mixing these water-soluble and biodegradable materials with better mechanical properties into drug solution, such that the microneedles can be totally dissolved and absorbed into the skin with no biohazardous waste needles left after administration. Furthermore, adequate drug loading can be achieved by adjusting the number of microneedles arranged in a patch.

The present study specifically focuses on dissolving microneedles array (DMNA) (19–21) for efficient transdermal delivery of sCT with higher therapeutic competence and better patient compliance (22). Based on the previous research (20) of optimizing the fabrication process of DMNA with improved needle drug proportion, we have prepared two formulations of sCT-dissolving microneedle array (sCT-DMNA-1 and sCT-DMNA-2) and thoroughly investigated their stability as well as *in vivo* bioavailability. We strongly believe that the study provides the research basis for further development of DMNs for other biotechnological drugs.

MATERIALS AND METHODS

Materials and Animals

sCT (purity > 99.47%, M_W = 3431.85) was purchased from Kaijie Biotechnology Co., Ltd. (Chendu, China). Dextran-40 (M_W = 40,000) and D-(+)-trehalose dihydrate (purity > 99%, M_W = 378.33) were procured from Shanghai Aladdin Biochemical Technology Co., Ltd. (Shanghai, China). PVP K90 (Kollidon® 90F, M_W = 630,000) was obtained from BASF SE (Ludwigshafen, Germany). *o*-cresolphthalein complex one (OCPC) colorimetric assay reagents and the other high-performance liquid chromatography (HPLC) grade solvents were purchased from Shanghai Aladdin Biochemical Technology Co., Ltd. (Shanghai, China).

Tibetan pig skins were obtained from the Experimental Animal Center of SunYat-sen University (Guangdong, China). Female Sprague-Dawley (SD) rats (Guangdong, China), weighing 180–220 g, were maintained under standard conditions with a 12-h light/dark cycle in the Experimental Animal Center of Sun Yat-sen University (Guangdong, China) for *in vivo* studies. All operations were approved by the Institutional Animal Care and Use Committee and were in accordance with the National Institutes of Health guidelines for the care and use of laboratory animals.

Fabrication of Molds

The master mold of DMNA was designed and manufactured by computer-aided micromilling technology. It is a brass model with a square matrix of 100 microneedles, shaped like a cone, and arranged in order of 10 × 10 arrays. Each needle was 800 μm long, 300 μm wide at the rounded base with 900 μm distances from the tip to tip. Polydimethylsiloxane (PDMS) monomer was mixed with the curing agent at a ratio of 10:1 (w/w), followed by vacuum degassing for 30 min. The mixture was then poured into the master mold and cured at a constant temperature of 80°C for 2 h. After cooling to room temperature, the PDMS female molds were peeled out of the master mold. DMNAs were prepared from PDMS female molds.

Preparation of sCT-DMNA

Table I demonstrates the formulations of Blank-DMNA and sCT-DMNAs (sCT-DMNA-1 and sCT-DMNA-2). Blank-DMNA solution was prepared by dissolving 25 mg Dextran in 50 μL deionized (DI) water. While sCT-DMNA-1 solution was prepared by mixing 2.5 mg sCT and 25 mg Dextran in 50 μL DI, sCT-DMNA-2 solution was prepared by dissolving 12.5 mg trehalose into the needle formulation of sCT-DMNA-1. The above solutions were stirred evenly and swelled overnight to form the needle solutions. Fifty milligrams of poly *N*-vinylpyrrolidone (PVP K90) was dissolved into 150 μL ethanol and swelled overnight to prepare the base solution (K90E). The delivery systems sCT-DMNAs were fabricated by the optimized two-step molding process in the previous

Table I. Formulations of Blank-DMNA and sCT-DMNAs

Formulation	sCT (mg)	Dextran 40 (mg)	Trehalose (mg)	H_2O (μL)	K90E (μL)
Blank-DMNA	-	25	-	50	150
sCT-DMNA-1	2.5	25	-	50	150
sCT-DMNA-2	2.5	25	12.5	50	150

research (20). An appropriate amount of sCT-DMNA-1/sCT-DMNA-2 solution was added onto the surface of PDMS female mold and centrifuged at 3000×*g* force for 10 min to make the solution enter into the micropores of the mold. The residual solution was then scraped off from the surface of the PDMS mold, and the drug-free solution, K90E, was casted onto the female mold, followed by centrifugation at 3000×*g* for another 5 min. After drying inside a desiccator at room temperature for 24 h, the sCT-DMNAs were stripped from the mold.

The micrographs of sCT-DMNAs were obtained employing a field emission scanning electron microscope (SEM) (JSM-6330F, Jeol, Tokyo, Japan) and an electron microscope (MP41, Mingmei, Guangdong, China).

Insertion Test of sCT-DMNAs in Pig Skin

The mechanical strength of sCT-DMNAs was evaluated by a texture analyzer (CT3, Brookfield, USA). The preserved frozen pig skins were thawed in normal saline and balanced for 30 min before wiping dry for the test. A piece of sCT-DMNA was fixed on the cylindrical probe of the texture analyzer; the probe was programmed to move straight to the stainless platform at the speed of 2 mm/s. As the microneedle touched the cuticle of the skin, the probe can detect the pressure change, then slowed down, and completely stopped till the pressure rose to 10 N (0.1 N/n), followed by holding for 30 s. After the probe moved away from the stainless platform, the skin was immediately dyed on the surface with 0.4% trypan blue solution for 10 min. The stain was then wiped off the surface, and the stained holes on the skin were counted to evaluate the cuticular penetration of sCT-DMNAs.

Needle Drug Loading Proportion in sCT-DMNAs

The loading amount of sCT in sCT-DMNAs was determined by HPLC (23) (LC-20AT binary pump, SPD-20A ultraviolet detector, SIL-20A autosampler, CBM-10A VP Plus detector, Shimadzu, Kyoto, Japan), employing a Jupiter 5u C18 column (250 × 4.6 mm i.d., 5 μm particle size, Phenomenex, Torrance, USA) at 220 nm. The needle and base part of sCT-DMNAs were separated with a surgical blade and dissolved in 1 mL PBS solution, which was prepared by mixing 0.87 g dipotassium hydrogen phosphate and 8.34 g potassium dihydrogen phosphate in 1000 mL ultrapure water. The mobile phases, containing tetramethylammonium hydroxide (A) and acetonitrile (B), were analyzed by dual gradient elution at the flow rate of 1 mL/min as shown in Table II. The column temperature was 30°C and the injection volume was 100 μL. The needle drug loading proportion (*NDP*) was obtained from the amount of drug in the needle part (M_n) and the amount in the base part (M_b). It was calculated by Eq. (1):

$$NDP\,(\%) = \frac{M_n}{M_n + M_b} \times 100\% \tag{1}$$

Table II. Time Program of Dual Gradient Elution

Time (min)	Mobile phase A (%)	Mobile phase B (%)
0	72	28
15	63	37
17	72	28
30	72	28

Stability of sCT-DMNAs

The stability study was performed by storing as-prepared sCT-DMNA-1, sCT-DMNA-2, and 50 g/mL sCT solution in the following four conditions: (a) low temperature with low humidity 4°C, 10% humidity (placed in a dryer inside a 4°C refrigerator); (b) room temperature with low humidity 25°C, 10% humidity (placed in a dryer at room temperature); (c) high temperature with low humidity 40°C, 10% humidity (placed in a drying oven at 40°C); (d) room temperature with high humidity 25°C, 55% humidity (placed in a drying vessel with high humidity at room temperature). The last environmental condition of high humidity was set by pouring supersaturated solution of silver nitrate at the bottom of the drying vessel, with sealing the drying vessel and the lid with Vaseline. After that, the drying vessel was placed at room temperature for 24 h and balanced to prepare 54.38 ± 0.23% relative humidity environment.

After 2 months of storage, sCT solution and sCT-DMNAs were taken out from the four environments for determining the sCT content by the method described in section 2.5.

In vivo Pharmacodynamics of sCT in Rats

Rats Hypocalcemic Test

To conduct hypocalcemic test, 52 female SD rats weighing 180–220 g were randomly assigned to seven groups after quarantined for 3 days. The control group (group 1) was only given jugular intubation, without any treatment. For the intravenous (IV) injection group (group 2), 0.2 mL sCT solution (100 μg/mL) was administered to the rats through neck vein injection. The subcutaneous injection group (group 3) was administered 0.2 mL sCT solution (100 μg/mL) through subcutaneous (SC) injection to alar skin. For the gels group (group 4), sCT-gel was daubed on the depilated area (2 cm × 2 cm) of abdominal skin, followed by covering with plastic wrap (Fig. 1b). The Blank-DMNA and sCT-DMNAs (groups 5–7) were administrated to the rats by the same operator on the inner side of the rat ears for 2 min with the same manual force, followed by holding in place for 2 h using special stainless steel clips (Fig. 1a). The treatment group (24–26) and the dosage are shown in Table III.

The animals were intraperitoneally injected with urethane solution (20%, w/v) at a dose of 0.6 mL/100 g for general anesthesia. The blood was then extracted by jugular vein catheterization (27). Samples of 200 μL blood were collected prior to administration of treatments as well as after administration of treatments at different time points (5, 15, 30, 45, 60, 90, 120, 180, 240, 360, 480, and 720 min). After keeping untouched for 1 h, the samples were centrifuged at 7000 rpm for 7 min to obtain the serum for analysis.

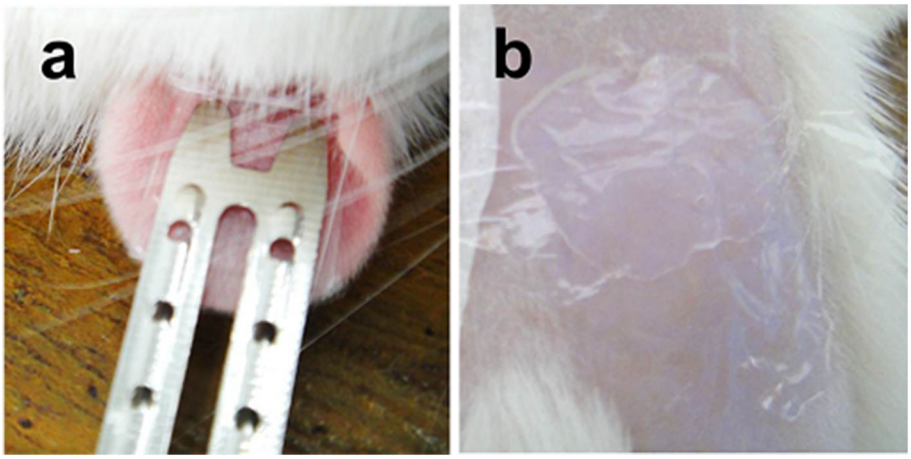

Fig. 1. Administration of DMNA (**a**) and sCT-gel on rats (**b**)

Serum Calcium Determination

Serum calcium concentration in plasma was determined by OCPC colorimetry (28). To conduct the assay, 8-hydroxyquinoline with final concentration of 2.2 mg/mL was added to the OCPC solution for eliminating the interference of magnesium ions in the samples (29). OCPC solution, diethylamine solution, and methanol were mixed at a ratio of 15:15:10 (v/v/v) to prepare calcium ion-chromogenic reagent prior to use.

The blank tube, standard tubes, and the sample tubes (obtained from "Rats Hypocalcemic Test") were prepared according to the procedure of Table IV. After placing for 5 min, the absorbance of OCPC complex was measured at 570 nm making the absorbance of the blank tube zero, using a dual beam UV-Visible spectrophotometer (TU-1901, Purkinje General Instrument Co., Beijing, China). The serum calcium concentration was obtained from the standard curve which was drawn by the concentration of standard solutions and their corresponding absorbances.

Data Processing and Pharmacodynamic Calculation

The serum calcium concentration of rats before treatment was used as the benchmark (100%), and the serum calcium relative concentration (F) at each point of time after treatment was calculated by the following Eq. (2):

$$F\ (\%) = \frac{C_i}{C_0} \times 100\% \tag{2}$$

where C_i represents the serum calcium concentration at the time of point i and C_0 represents the serum calcium concentration before treatment. The serum calcium relative concentration-time curve was plotted with $F(\%)$ *vs.* the time point. The trapezoidal method (30) was used to calculate the area under concentration-time curve (AUC) of serum calcium, as shown in Eq. (3):

$$AUC = \frac{\sum (T_i - T_{i-1}) \times (F_{i-1} + F_i)}{2} \tag{3}$$

where T_i and F_i represent the time value and the percentage value of serum calcium relative concentration corresponding to the i-th blood sampling point, respectively. AUC is the sum of the trapezoidal areas formed of all adjacent points and the X-axis.

Hypocalcemic effect (D) and relative bioavailability (PA) were calculated by the following Eqs. (4) and (5), respectively.

$$D\ (\%) = \frac{AUC_c - AUC_x}{AUC_c} \times 100\% \tag{4}$$

$$PA\ (\%) = \frac{D_x \times \mathrm{Dose}_{sc}}{D_{sc} \times \mathrm{Dose}_x} \times 100\% \tag{5}$$

Table III. The Treatment Group of Rats and the Dosage in Terms of sCT

Group	Number	Treatment	sCT dosage (μg)
1	7	Control	-
2	7	IV	20
3	7	SC	20
4	7	sCT-gel	40
5	8	Blank-DMNA	-
6	8	sCT-DMNA-1	~ 41.31
7	8	sCT-DMNA-2	~ 39.56

Table IV. Determination Procedure of Serum Calcium

Adding material	Blank tube	Standard tube	Sample tube
Ca^{2+} standard solution	-	50 μL	-
Serum	-	-	50 μL
Purified water	100 μL	50 μL	50 μL
Chromogenic reagent	4 mL	4 mL	4 mL

where AUC_x is the AUC value of each agent and the positive control and AUC_c is the AUC value of the negative control corresponding to AUC_x preparation. D_x and $Dose_x$ represent the hypocalcemic effect and dose of sCT-DMNA and sCT-gel, respectively. D_{sc} and $Dose_{sc}$ refer to the hypocalcemic effect and dose of sCT-solution (SC), respectively.

Statistical Analysis

The results were presented as mean ± standard deviation between values were analyzed using SPSS Statistics 22.0 (IBM, New York, USA) for windows 7. The values of individual groups were operated by Student's t test for comparison. The difference was regarded statistically significant if $p < 0.05$.

RESULTS

Analytical Characterization of sCT-DMNA

The SEM (Fig. 2a) and electron micrographs (Fig. 2b) of sCT-DMNA are shown in Fig. 2. The micrographs observed under SEM and electron microscope clearly demonstrate that the two kinds of sCT-DMNAs possess the neat shape and are in good agreement with that of the mold.

The mechanical properties of sCT-DMNA-1 and sCT-DMNA-2 were examined *in vitro* using pig skin. Three samples were detected for both sCT-DMNA-1 and sCT-DMNA-2. The results exhibited that the sCT-DMNAs could achieve more than 95% cuticular penetration (Fig. 3).

Drug Loading and NDP of sCT-DMNAs

The drug loading amount of sCT-DMNA-1 patch was 48.06 ± 6.08 μg, and the effective drug loading of the needle part was about 41.31 μg, with the NDP 85.96%. The total drug loading of sCT-DMNA-2 (containing trehalose) patch was 46.10 ± 5.46 μg, and the effective drug loading of the needle part was approximately 39.56 μg, with the NDP 85.81%. From the above results, it can be comprehended that the stabilizer trehalose had no significant effect ($p > 0.05$) on the drug loading and NDP of sCT-DMNA.

Stability Study of sCT-DMNAs

The initial drug loading in sCT-DMNAs and the drug loading after 2 months of storage at different environmental conditions are shown in Fig. 4. While no sCT was detected in the sCT solution under the four conditions after 2 months of storage, sCT was detected in sCT-DMNAs samples under the above four conditions. The result indicates that the stability of sCT encapsulated in DMNAs was much better as compared with free sCT in solution, and the preparation of sCT-DMNA was conducive to the stability of polypeptide drug sCT.

For sCT-DMNA-1, the concentration of sCT in patch did not decrease significantly after 2 months of storage at room temperature with low humidity. Although the concentration of sCT was decreased at low temperature with low humidity, there was no statistical difference with the initial drug loading. Therefore, it can be stated that these two conditions were suitable for the storage of sCT-DMNA-1 patch, and room temperature with low humidity is more favorable. Contrastingly, at the storage conditions of room temperature with high humidity and high temperature with low humidity, the drug loadings of sCT-DMNA-1 were drastically reduced (even lower than 60% of the initial drug loading), with statistically significant difference ($p < 0.05$). The above results demonstrate that the temperature and humidity are the main factors that could hamper the stability of sCT-DMNA-1.

The sCT-DMNA-2 patch, containing trehalose (Tre) in the excipients, was stored under four conditions as well. After 2 months of storage, there was no statistical difference in the change of drug loading. At room temperature with low humidity and at low temperature with low humidity, the drug loading did not decrease significantly, confirming again that these two conditions are suitable for the storage of sCT-DMNAs. Moreover, at room temperature with high humidity and high temperature with low humidity, the drug loadings of sCT-DMNA-2 were only slightly decreased, in comparison with those of sCT-DMNA-1 which were drastically reduced, the differences were statistically significant ($p < 0.05$), indicating that the trehalose could enhance the chemical stability of sCT encapsulated in DMNA.

In vivo Pharmacodynamics

Two negative controls (group 1 and group 5) were set for the pharmacodynamic study. The control group without any treatment (group 1) was used to compare with other groups to eliminate the possible influence of jugular vein intubation on blood calcium level. On the other hand, the blank microneedle group (group 5) was compared with the microneedle administration groups to eradicate the possible effect of microneedle insertion and dissolution of microneedle

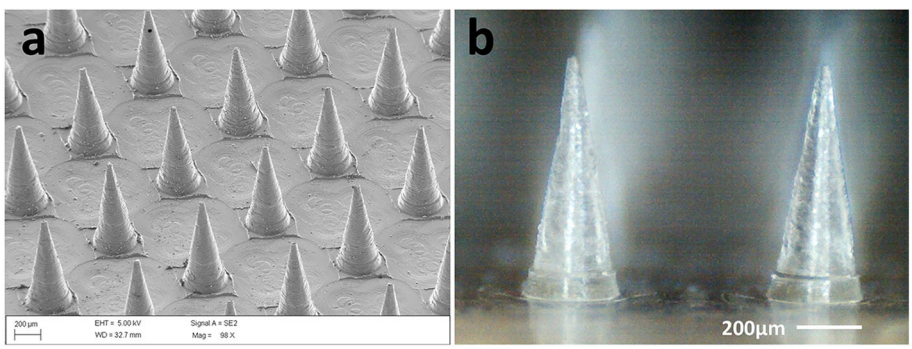

Fig. 2. Images of sCT-DMNA photographed by SEM (**a**) and an electron microscope (**b**)

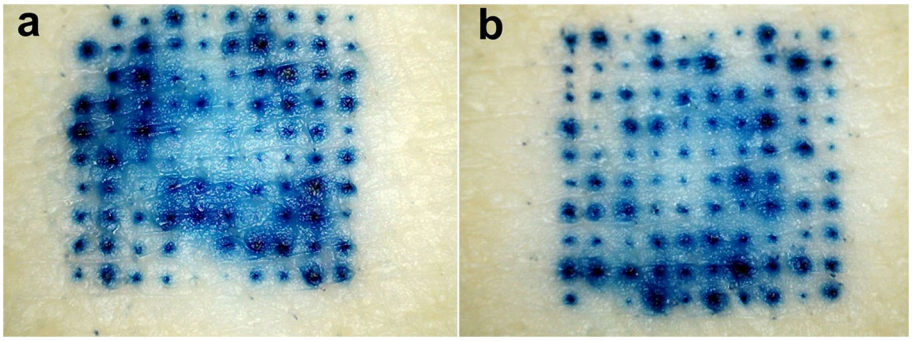

Fig. 3. Skin penetration of sCT-DMNA-1 (**a**) and sCT-DMNA-2 (**b**)

excipients on blood calcium level. Intravenous injection (IV, group 2) and subcutaneous injection (SC, group 3) of sCT solution were used as positive control groups.

Relative Serum Calcium Concentration in Rats vs. Time Curve

The profiles of relative serum calcium concentration with time for control groups are shown in Fig. 5a. The two curves of the negative control groups were relatively close, with no statistical difference, suggesting that microneedle insertion and excipients had little effect on blood calcium level of rats. The serum calcium relative concentrations ($F\%$) of both the curves were reduced slightly within the first 1 h, followed by gradual recovery and finally maintained at the baseline level. The results indicate that jugular intubation could lead to a brief drop of serum calcium concentration in rats and the effect can be basically eliminated within 2 h. The respective curves of two positive control groups (IV and SC) had a good coincidence degree with each other, and the serum calcium levels of the groups were decreased very fast up to first 3 h and then remained at a lower level with significant difference ($p < 0.05$) to the curves of the negative control groups. The results altogether demonstrate that the efficacy of SC injection was similar to that of IV injection, both of which had significant effect of hypocalcemia. Moreover, the minor effect of serum calcium from jugular intubation did not affect the overall outcome of the experiment.

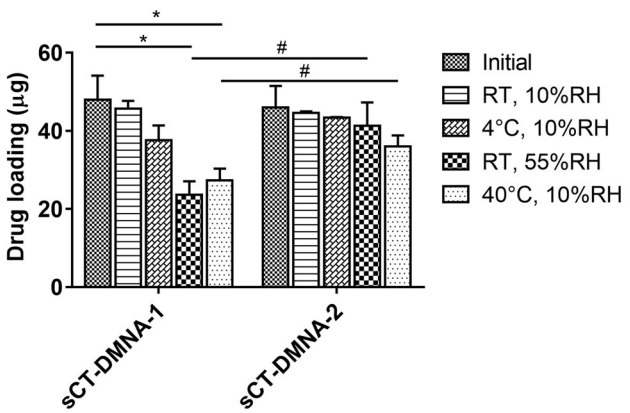

Fig. 4. The change of drug loading after 2-month storage of sCT-DMNAs at four different environmental conditions. The data are represented as the mean of independent experiments, with the vertical bars indicating the standard deviation ($n = 3$). $^{*}p < 0.05$ *vs.* the initial drug loading of sCT-DMNA-1. $^{\#}p < 0.05$ *vs.* the same group of sCT-DMNA-1

The respective curve of gel group was found in between the curves of Control group (negative control group) and SC group (positive control group), as shown in Fig. 5b. The curve of gel group was relatively close to that of the negative control group, and there was no statistical difference among the corresponding points ($p > 0.05$). However, the curve of gel group was far apart from the curve of positive control group and there was a statistically significant difference ($p < 0.05$) at each point after 3 h time points, indicating that the efficacy of sCT-gel administration to the rats was not significant.

As shown in Fig. 5c, the respective curves of sCT-DMNA-1 and sCT-DMNA-2 groups had a good coincidence degree with the curve of SC group (the positive control group), with no statistical difference at all the points ($p > 0.05$). It can be inferred here that the pharmacodynamic difference between sCT-DMNAs and SC groups could not be distinguished only from the curve. However, it can be stated that sCT-DMNAs had significant hypocalcemic effect ($p < 0.05$) as compared with the Blank-DMNA group.

Hypocalcemic Effects and Relative Bioavailability

The hypocalcemic effects and pharmacologically relative bioavailability of each experimental group were calculated according to relevant formulas and are shown in Table V. The dose of sCT-DMNAs in the table was the actual release dose calculated by the initial dose minus the residual dose in the sCT-DMNAs patch after administration.

According to the results in Table V, the hypocalcemic effects ($D\%$) of two positive control groups IV and SC were similar, which is consistent with the results of Fig. 5a, further suggesting that similar hypocalcemic effect could be achieved by SC and IV routes of sCT administration. The hypocalcemic effects of sCT-DMNAs were close to that of the positive control groups, and the relative bioavailabilities of pharmacology ($PA\%$) for both the sCT-DMNA-1 and sCT-DMNA-2 were approximately 70%, suggesting that sCT-DMNAs had the ideal hypocalcemic effect and higher relative bioavailability. The hypocalcemic effect ($D\%$) of the gel group was significantly lower than that of the positive control groups and sCT-DMNAs groups ($p < 0.01$), with relative bioavailability ($PA\%$) only 11%, which was approximately one-sixth times less than that of sCT-DMNA-2. The results indicate that DMNA could significantly improve the therapeutic effects of polypeptide drug sCT in comparison with the conventional transdermal delivery system (gel patch).

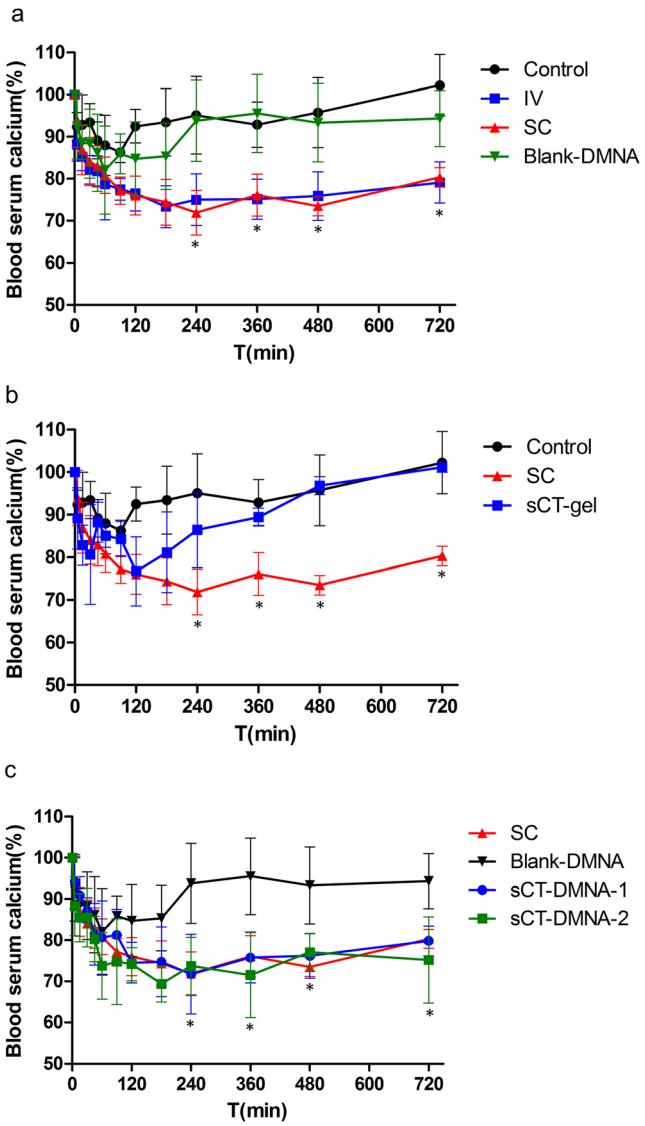

Fig. 5. Relative blood serum calcium concentration *vs.* time profiles after administration of different treatments. Statistical significance for comparison of individual groups was determined by Student's *t* test. **a** The profiles for control groups (negative control: control and Blank-DMNA, positive control: IV injection and SC injection of sCT). $*p < 0.05$ *vs.* the curves of the negative control groups at each point after 3 h time points. **b** Serum calcium concentration after administration of sCT-gel (negative control: Control, positive control: SC injection of sCT). $*p < 0.05$ *vs.* the curve of sCT-gel group at each point after 3 h time points. **c** Serum calcium concentration after administration of sCT-DMNAs (negative control: Blank-DMNA, positive control: SC injection of sCT). $*p < 0.05$ *vs.* the curve of Blank-DMNA group at each point after 3 h time points

The initial drug loading of sCT-DMNA-2 (initial drug loading 39.6 μg, release dose 30.0 μg), containing the stabilizer trehalose, was found to be slightly lower as compared with that of sCT-DMNA-1 (initial drug loading 41.3 μg, release dose 27.5 μg). On the other hand, the actual release dose, corresponding hypocalcemic effect, and relative bioavailability of sCT-DMNA-2 were higher than that of sCT-DMNA-1. The results indicate that the presence of trehalose in the sCT-DMNA could improve the transdermal release of sCT leading to obtain higher hypocalcemic effect.

DISCUSSION

Effective Distribution of sCT in sCT-DMNAs

During the preparation and solidification process of sCT-DMNAs, the drug, encapsulated in the needle portion diffusing (31,32) to the base, directly leads to the reduction of NDP. In our previous report (20), the factors affecting the NDP of the drug-containing DMNA were thoroughly investigated. The solvent evaporation from the base solution was found to be the key factor to suppress the drug diffusion from the needle to the base. It was observed that the drug diffusion rate was dramatically reduced due to the rapid evaporation of ethanol, which resulted in a sharp increase in the viscosity of the base layer. In the present study, DI water was used as the needle solvent and highly volatile ethanol as the base solvent for two-step injection in mold, followed by rapid drying process, leading to significantly increase in the NDP of sCT-DMNAs. The NDPs of sCT-DMNA-1 and sCT-DMNA-2 were 85.96% and 85.81%, respectively.

Improvement in Stability and Hypocalcemia Effect

In order to increase the stability of the peptide in the microneedles, we considered addition of trehalose to the excipients. Trehalose is a reductive disaccharide that consists of two glucose units linked by an α, α-(1 → 1)-linkage. Trehalose is found in natural organisms, where it can not only replace water molecules by forming hydrogen bonds with polar residues of lipid and/or protein molecules (water substitution hypothesis) (33,34) but also act as a protector against various stress conditions including freeze, osmotic stress, oxidation, and changes in temperature (35).

The spatial structure of peptides and proteins is primarily maintained by secondary bonds such as hydrogen bonds. At adverse conditions including high temperature and humidity, the secondary bonds can be destroyed and the polypeptide is unfolded. The hydrophobic groups originally in the interior of molecules are largely exposed to the molecular surface (36,37). Fortunately, the presence of trehalose as a chemical chaperone stabilizes the denatured peptides and facilitates their refolding *in vivo* and *in vitro* (38–40). Therefore, trehalose as a part of the needle excipients could make sCT-DMNA-2 still maintain a good stability after being stored in adverse environmental conditions of high temperature and high humidity for 2 months; as shown in Fig. 4, the effective concentration of sCT in sCT-DMNA-2 did not decrease significantly as compared with the initial concentration, whereas its values were significantly different ($p < 0.05$) from that of sCT-DMNA-1 group (without trehalose) with the drug loadings reducing less than 60%.

In vivo pharmacodynamic study demonstrates that the hypocalcemic effect for sCT-DMNA-2 was slightly higher than that of sCT-DMNA-1, which was consistent with their release dose, while the initial drug loading of sCT-DMNA-2 (initial drug loading 39.6 μg, release dose 30.0 μg), containing trehalose, was slightly lower as compared with that of sCT-DMNA-1 (initial drug loading 41.3 μg, release dose 27.5 μg), as shown in Table V. This result indicates that trehalose can improve the hypocalcemia effect of sCT. The reason may be that the existence of trehalose accelerates the needle dissolution speed of sCT-DMNA-2 when

Table V. Hypocalcemic Effects and Pharmacologically Relative Bioavailability of Each Group

Group	*AUC*	Dosage (μg)	*D* (%)	*PA* (%)
Control	68,373.6 ± 3770.6	-	-	-
IV	55,280.5 ± 2241.3	20.0	19.1 ± 3.3	-
SC	55,023.9 ± 1557.0	20.0	19.5 ± 2.3	-
sCT-gel	65,394.0 ± 2301.8	40.0	4.3 ± 3.4	11.3 ± 6.2
Blank-DMNA	66,044.0 ± 4821.5	-	-	-
sCT-DMNA-1	55,553.3 ± 3250.6	27.5 ± 3.7	18.8 ± 4.8	71.2 ± 18.1
sCT-DMNA-2	53,983.1 ± 3388.4	30.0 ± 3.5	21.0 ± 5.0	73.3 ± 17.3

Results are presented as mean ± standard deviation

the microneedles penetrated the epidermis, thus improving the drug release amount, due to the high hydrophilicity (41) of trehalose (solubility in water: trehalose ≈ 689 mg/mL, dextran ≈ 50 mg/mL, 20°C).

CONCLUSION

To investigate the feasibility and *in vivo* pharmacological activity of DMNA patches for non-injection administration of biomacromolecule drugs, two formulations of sCT-DMNA patches (sCT-DMNA-1 and sCT-DMNA-2) were prepared. The results demonstrated that the mechanical properties and the drug distributions of the DMNA patches met all the requirements for transdermal administration. *In vivo* pharmacodynamics further confirmed that sCT-DMNAs could achieve similar hypocalcemic effects to subcutaneous injection of sCT and significantly enhance the relative bioavailability of drug as compared with the conventional transdermal delivery system sCT-gels. Comparing the results of the two sCT-DMNA formulations, it was observed that sCT-DMNA-2 containing trehalose was more conducive to the stability and transdermal delivery of sCT. In conclusion, we strongly believe that the sCT-DMNA patches could be employed for the efficient delivery of sCT for the treatment of bone disorders in near future.

AUTHOR CONTRIBUTIONS

Lu Zhang: conceptualization, methodology, software, investigation, writing—original draft.
Yingying Li: validation, formal analysis, visualization, software.
Fang Wei: validation, formal analysis, visualization.
Hang Liu: resources, writing—review and editing, supervision, data curation.
Yushuai Wang: resources, writing—review and editing, supervision, data curation.
Weiman Zhao: resources, writing—review and editing, supervision.
Zhiyong Dong: writing—review and editing.
Tao Ma: writing—review and editing.
Qingqing Wang: writing—review and editing.

FUNDING

This work was supported by the National Natural Science Foundation of China (Grant No. 81502994), Key Projects of Outstanding Young Talents Support Program in universities of Anhui Province (Grant No. gxyqZD2020026), and Natural Science Foundation of Anhui Province (Grant No. 1608085QH179).

COMPLIANCE WITH ETHICAL STANDARDS

All operations were approved by the Animal Ethical Committee of Sun Yat-sen University and were in accordance with the National Institutes of Health guidelines for the care and use of laboratory animals.

Conflict of Interest The authors declare that there are no competing interests.

REFERENCES

1. Huang CLH, Sun L, Moonga BS, Zaidi M. Molecular physiology and pharmacology of calcitonin. Cell Mol Biol (Noisy-le-grand). 2006;52(3):33–43.
2. Naot D, Musson DS, Cornish J. The activity of peptides of the calcitonin family in bone. Physiol Rev. 2019;99(1):781–805. https://doi.org/10.1152/physrev.00066.2017.
3. Bandeira L, Lewiecki EM, Bilezikian JP. Pharmacodynamics and pharmacokinetics of oral salmon calcitonin in the treatment of osteoporosis. Expert Opin Drug Metab Toxicol. 2016;12(6):681–9. https://doi.org/10.1080/17425255.2016.1175436.
4. Allison SL, Davis KW. Calcitonin stewardship strategies. J Pharm Pract. 2019;32:584–5. https://doi.org/10.1177/0897190018770052.
5. Ito A, Yoshimura M. Mechanisms of the analgesic effect of calcitonin on chronic pain by alteration of receptor or channel expression. Mol Pain. 2017;13:1744806917720316. https://doi.org/10.1177/1744806917720316.
6. Okabe K, Okamoto F, Kajiya H. Odontoclasts and calcitonin. Clin Calcium. 2012;22:19–26 CliCa12011926 (DOI Not Found).
7. Bajracharya R, Song JG, Back SY, Han HK. Recent advancements in non-invasive formulations for protein drug delivery. Comput Struct Biotechnol J. 2019;17:1290–308. https://doi.org/10.1016/j.csbj.2019.09.004.
8. Putney SD, Burke PA. Improving protein therapeutics with sustained-release formulations. Nat Biotechnol. 1998;16:153–7. https://doi.org/10.1038/nbt0298-153.
9. Torres-Lugo M, Peppas NA. Transmucosal delivery systems for calcitonin: a review. Biomaterials. 2000;21:1191–6. https://doi.org/10.1016/S0142-9612(00)00011-9.

10. Sun L, Le Z, He S, Liu J, Liu L, Leong KW, et al. Flash fabrication of orally targeted nanocomplexes for improved transport of salmon calcitonin across the intestine. Mol Pharm. 2020;17:757–68. https://doi.org/10.1021/acs.molpharmaceut.9b00827.
11. Liu L, Yang H, Lou Y, Wu JY, Miao J, Lu XY, et al. Enhancement of oral bioavailability of salmon calcitonin through chitosan-modified, dual drug-loaded nanoparticles. Int J Pharm. 2019;557:170–7. https://doi.org/10.1016/j.ijpharm.2018.12.053.
12. Onishi H, Tokuyasu A. Preparation and evaluation of enteric-coated chitosan derivative-based microparticles loaded with salmon calcitonin as an oral delivery system. Int J Mol Sci. 2016;17(9):1546. https://doi.org/10.3390/ijms17091546.
13. Asafo-Adje TA, Chen AJ, Najarzadeh A, Puleo DA. Advances in controlled drug delivery for treatment of osteoporosis. Curr Osteoporos Rep. 2016;14(5):226–38. https://doi.org/10.1007/s11914-016-0321-4.
14. Pontiroli AE. Peptide hormones: review of current and emerging uses by nasal delivery. Adv Drug Deliv Rev. 1998;29:81–7. https://doi.org/10.1016/S0169-409X(97)00062-8.
15. Manosroi J, Lohcharoenkal W, Götz F, Werner RG, Manosroi W, Manosroi A. Transdermal absorption and stability enhancement of salmon calcitonin by Tat peptide. Drug Dev Ind Pharm. 2013;39(4):520–5. https://doi.org/10.3109/03639045.2012.684388.
16. Amaro MI, Tewes F, Gobbo O, Tajber L, Corrigan OI, Ehrhardt C, et al. Formulation, stability and pharmacokinetics of sugar-based salmon calcitonin-loaded nanoporous/nanoparticulate microparticles (NPMPs) for inhalation. Int J Pharm. 2015;483(1–2):6–18. https://doi.org/10.1016/j.ijpharm.2015.02.003.
17. Tas C, Mansoor S, Kalluri H, Zarnitsyn VG, Choi SO, Banga AK, et al. Delivery of salmon calcitonin using a microneedle patch. Int J Pharm. 2012;423(2):257–63. https://doi.org/10.1016/j.ijpharm.2011.11.046.
18. Vemulapalli V, Bai Y, Kalluri H, Herwadkar A, Kim H, Davis SP, et al. In vivo Iontophoretic delivery of salmon calcitonin across microporated skin. J Pharm Sci. 2012;101(8):2861–9. https://doi.org/10.1002/jps.23222.
19. Gomaa YA, Garland MJ, McInnes F, El-K LK, Wilson C, Donnelly RF. Laser-engineered dissolving microneedles for active transdermal delivery of nadroparin calcium. Eur J Pharm Biopharm. 2012;82(2):299–307. https://doi.org/10.1016/j.ejpb.2012.07.008.
20. Wang Q, Yao G, Dong P, Gong Z, Li G, Zhang K, et al. Investigation on fabrication process of dissolving microneedle arrays to improve effective needle drug distribution. Eur J Pharm Sci. 2015;66:148–56. https://doi.org/10.1016/j.ejps.2014.09.011.
21. Yao G, Quan G, Lin S, Peng T, Wang Q, Ran H, et al. Novel dissolving microneedles for enhanced transdermal delivery of levonorgestrel: in vitro and in vivo characterization. Int J Pharm. 2017;534:378–86. https://doi.org/10.1016/j.ijpharm.2017.10.035.
22. Herwadkar A, Banga AK. Peptide and protein transdermal drug delivery. Drug Discov Today Technol. 2011;9(2):e71–e174. https://doi.org/10.1016/j.ddtec.2011.11.007.
23. Cetin M, Youn YS, Capan Y, Lee KC. Preparation and characterization of salmon calcitonin-biotin conjugates. AAPS PharmSciTech. 2008;9(4):1191–7. https://doi.org/10.1208/s12249-008-9165-2.
24. Sun P, Zhang X, Chen Y, Zang X. Application of the yeast-surface-display system for orally administered salmon calcitonin and safety assessment. Biotechnol Prog. 2010;26(4):968–74. https://doi.org/10.1002/btpr.413.
25. Karsdal MA, Byrjalsen I, Henriksen K, Riis BJ, Christiansen C. A pharmacokinetic and pharmacodynamic comparison of synthetic and recombinant oral salmon calcitonin. J Clin Pharmacol. 2009;49(2):229–34. https://doi.org/10.1177/0091270008329552.
26. Millest AJ, Evans JR, Young JJ, Johnstone D. Sustained release of salmon calcitonin in vivo from lactide: glycolide copolymer depots. Calcif Tissue Int. 1993;52(5):361–4. https://doi.org/10.1007/BF00310200.
27. Feng J, Fitz Y, Li Y, Fernandez M, Cortes PI., Wang D, et al. Catheterization of the carotid artery and jugular vein to perform hemodynamic measures, infusions and blood sampling in a conscious rat model. J Vis Exp. 2015;30(95). https://doi.org/10.3791/51881.
28. Hartmann AE, Lewis LR. Evaluation of the ASTRA o-cresolphthalein complexone calcium method. Am J Clin Pathol. 1984;82(2):182–7. https://doi.org/10.1093/ajcp/82.2.182.
29. Cohen SA, Sideman L. Modification of the o-cresolphthalein complexone method for determining calcium. Clin Chem. 1979;25(8):1519–20.
30. Zhang T, Heimbach T, Lin W, Zhang J, He H. Prospective predictions of human pharmacokinetics for eighteen compounds. J Pharm Sci. 2015;104(9):2795–806. https://doi.org/10.1002/jps.24373.
31. Lock JY, Carlson TL, Carrier RL. Mucus models to evaluate the diffusion of drugs and particles. Adv Drug Deliv Rev. 2018;124(15):34–49. https://doi.org/10.1016/j.addr.2017.11.001.
32. Okamura E. Solution NMR to quantify mobility in membranes: diffusion, protrusion, and drug transport processes. Chem Pharm Bull. 2019;67(4):308–15. https://doi.org/10.1248/cpb.c18-00946.
33. Crowe LM. Lessons from nature: the role of sugars in anhydrobiosis. Comp Biochem Physiol. 2002;131A:505–13. https://doi.org/10.1016/S1095-6433(01)00503-7.
34. Crowe JH, Hoekstra FA, Crowe L. Anhydrobiosis. Annu Rev Physiol. 1992;54:579–99. https://doi.org/10.1146/annurev.ph.54.030192.003051.
35. Elbein AD, Pan YT, Pastuszak I, Carroll D. New insights on trehalose: a multi functional molecule. Glycobiology. 2003;13:17–27. https://doi.org/10.1093/glycob/cwg047.
36. Oliveira IP, Martínez L. The shift in urea orientation at protein surfaces at low pH is compatible with a direct mechanism of protein denaturation. Phys Chem Chem Phys. 2019;22(1):354–67. https://doi.org/10.1039/c9cp05196a.
37. Diamant S, Eliahu N, Rosenthal D, Goloubin P. Chemical chaperones regulate molecular chaperones in vitro and in cells under combined salt and heat stresses. J Biol Chem. 2001;276:39586–91. https://doi.org/10.1074/jbc.M103081200.
38. Welch WJ, Brown CR. Influence of molecular and chemical chaperones on protein folding. Cell Stress Chaperones. 1996;1:109–15. https://doi.org/10.1379/1466-1268(1996)001<0109:iomacc>2.3.co;2.
39. Singer MA, Lindquist S. Multiple effects of trehalose on protein folding in vitro and in vivo. Mol Cell. 1998;1:639–48. https://doi.org/10.1016/s1097-2765(00)80064-7.
40. Corradini D, Strekalova EG, Stanley HE, Gallo P. Microscopic mechanism of protein cryopreservation in an aqueous solution with trehalose. Sci Rep. 2013;3:1218. https://doi.org/10.1038/srep01218.
41. Laskowska E, Kuczyńska-Wiśnik D. New insight into the mechanisms protecting bacteria during desiccation. Curr Genet. 2020;66(2):313–8. https://doi.org/10.1007/s00294-019-01036-z.